

Thermalization and photoluminescence dynamics of indirect excitons at low bath temperatures

This article has been downloaded from IOPscience. Please scroll down to see the full text article.

2004 J. Phys.: Condens. Matter 16 S3629

(<http://iopscience.iop.org/0953-8984/16/35/005>)

View [the table of contents for this issue](#), or go to the [journal homepage](#) for more

Download details:

IP Address: 129.252.86.83

The article was downloaded on 27/05/2010 at 17:18

Please note that [terms and conditions apply](#).

Thermalization and photoluminescence dynamics of indirect excitons at low bath temperatures

A L Ivanov

Department of Physics and Astronomy, Cardiff University, PB 913, 5 The Parade,
Cardiff CF24 3YB, UK

Received 6 July 2004

Published 20 August 2004

Online at stacks.iop.org/JPhysCM/16/S3629

doi:10.1088/0953-8984/16/35/005

Abstract

The thermalization and photoluminescence (PL) dynamics of indirect excitons in GaAs/AlGaAs coupled quantum wells (QWs) at very low bath temperature, $T_b < 1$ K, are analysed theoretically and modelled numerically in order to clarify the origin of the recently observed sharp increase of the PL signal (PL-jump) right after a high-intensity excitation pulse. We conclude that the PL-jump effect is mainly due to classical cooling of indirect excitons after the pump pulse, which heats the exciton system. Thus the effect cannot unambiguously be attributed to bosonic stimulation of the scattering processes into the ground-state mode $\mathbf{p}_{\parallel} = 0$. It is argued that the narrowing effect, i.e. an effective screening of in-plane QW disorder by dipole–dipole interacting indirect excitons, naturally explains the observed strongly nonlinear dependence of the PL rise time on the pump intensity. We also discuss and analyse an evaporative optical heating/cooling effect: the change of the effective temperature T of indirect excitons, due to their resonant optical decay.

1. Introduction

At present there are a lot of research activities searching for Bose–Einstein condensation (BEC) or BEC-like phase transitions of QW excitons or microcavity polaritons in GaAs-based nanostructures [1]. A system of indirect excitons in GaAs/AlGaAs coupled quantum wells is a unique candidate for the experimental realization of nonclassical, Bose–Einstein (BE) statistics for quasi-two-dimensional (quasi-2D) composite bosons with a well-defined in-plane momentum of the translational motion. This is due to a long radiative lifetime of the particles and effective screening of QW disorder by dipole–dipole interacting indirect excitons.

For a dilute (quasi-) equilibrium gas of QW excitons the degeneracy temperature T_0 and chemical potential μ_{2d} are given by

$$T_0 = \frac{2\pi}{g} \left(\frac{\hbar^2}{M_x} \right) n_{2d} \quad \text{and} \quad \mu_{2d} = k_B T \ln(1 - e^{-T_0/T}), \quad (1)$$

where g , M_x , n_{2d} and T are the spin-degeneracy factor, in-plane translational mass, concentration and temperature of excitons, respectively. For indirect excitons in GaAs coupled QWs the exchange interaction is extremely weak, so that $g = 4$. In the presence of a strong magnetic field H_\perp applied perpendicularly to the QW plane (the case we also analyse in this paper), the in-plane exciton mass becomes H_\perp -dependent, $M_x = M_x(H_\perp)$, and removal of the spin degeneracy occurs, i.e. $g = 1$. A crossover from classical to quantum, BE statistics takes place at $T \simeq T_0$. The distribution function of QW excitons, normalized to give a total number of particles, is

$$N_E = \frac{1 - e^{-T_0/T}}{e^{E/k_B T} + e^{-T_0/T} - 1}, \quad (2)$$

where $E = (\hbar^2 p_\parallel^2)/(2M_x)$ and $\hbar \mathbf{p}_\parallel$ is the in-plane momentum. According to equation (2), the occupation number of the ground-state mode $\mathbf{p}_\parallel = 0$ is

$$N_{\mathbf{p}_\parallel=0} \equiv N_{E=0} = e^{T_0/T} - 1. \quad (3)$$

For $T \ll T_0$, equations (1) and (3) yield $\mu_{2d} \simeq -k_B T e^{-T_0/T} \rightarrow 0$ and exponential, explosive population of the ground state mode with decreasing T . This can probably initiate BEC (in a finite-size, mesoscopic in-plane trap) or BEC-like phase transitions.

A strong increase of the PL signal from nonresonantly photogenerated indirect excitons, right after a rectangular pump pulse, was observed in optical experiments with GaAs coupled QWs at $0.05 \text{ K} \leq T_b \leq 15 \text{ K}$ [2, 3]. In particular, for the extremely low cryostat temperature $T_b = 50 \text{ mK}$, reported in [3], a phonon vacuum is nearly realized for LA-phonons involved in the thermalization of indirect excitons. The above effect of transient rise of resonant photoluminescence from indirect excitons is called a PL-jump. The observed nonlinear behaviour of the PL-jump, against the optical pump intensity, has mainly been interpreted in terms of stimulated scattering of excitons into the low-energy states with $\mathbf{p}_\parallel \simeq 0$ [3]. According to the experiments, the PL-jump effect disappears with increasing bath temperature T_b and with decreasing maximum density of indirect excitons, n_{2d}^{max} (i.e. with decreasing pump intensity).

Indirect magnetoexcitons in GaAs/AlGaAs coupled QWs [4–6] provide us with an additional degree of freedom in studying the relaxation and PL dynamics. In particular, the in-plane translational mass of indirect excitons can be considerably enhanced by applying a strong magnetic field perpendicular to the quantum wells: $M_x = M_x(H_\perp)$ increases with increasing H_\perp . According to the experiments [2, 3], the PL-jump contrast decreases with increasing H_\perp .

In the first optical experiments [7, 8] with indirect excitons in GaAs coupled QWs the inhomogeneous linewidth of the PL signal was large, $\hbar \Gamma_{\text{inhom}} \simeq 3\text{--}6 \text{ meV}$, i.e. even larger than the exciton binding energy, $\epsilon_x = 3\text{--}5 \text{ meV}$ [9]. In current high-quality structures an average inhomogeneous broadening is $\hbar \Gamma_{\text{inhom}} \simeq 0.7\text{--}1 \text{ meV}$, i.e. much less than ϵ_x . As it is shown in [10] and in the present paper, Γ_{inhom} can further be considerably reduced for $n_{2d} \geq 10^{10} \text{ cm}^{-2}$, due to the screening of QW disorder by dipole–dipole interacting indirect excitons. This justifies the thermodynamic description with equations (1)–(3), i.e. the description given in terms of a well-defined in-plane momentum \mathbf{p}_\parallel even for low-energy indirect excitons.

In this paper we study relaxation and PL dynamics of indirect excitons in GaAs-based coupled QWs at very low T_b , aiming

- (i) to understand the origin of the PL-jump and, in particular, to clarify to what extent this effect can be attributed to bosonic stimulation of exciton scattering,
- (ii) to discuss the screening of QW disorder by dipole–dipole interacting excitons and to show that for $n_{2d} \geq 10^{10} \text{ cm}^{-2}$ and low T the in-plane random potential is strongly weakened, and

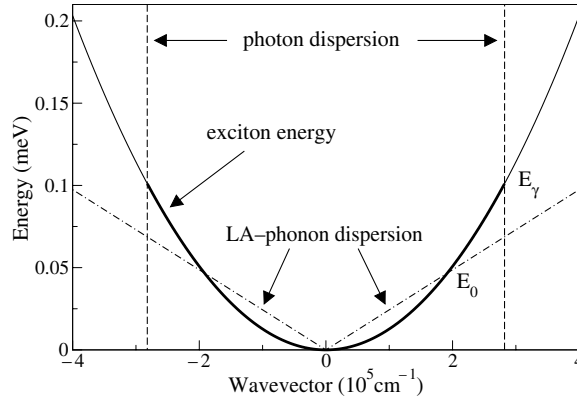


Figure 1. Schematic of the single-particle energies relevant to the relaxation and PL dynamics of indirect excitons in GaAs/AlGaAs coupled quantum wells. The exciton dispersion is $\hbar\omega_x = \hbar\omega_t + E(p_{\parallel})$, where $E = (\hbar^2 p_{\parallel}^2)/(2M_x)$ is the exciton kinetic energy (solid curve); the photon dispersion, $\hbar\omega_{\gamma} - \hbar\omega_t = (\hbar c p)/\sqrt{\varepsilon_b} - \hbar\omega_t$, is shown by the dashed lines; the LA-phonon dispersion, $\hbar\omega_{LA} = \hbar v_s p$, is shown by the dash-dotted lines. The low-energy exciton states, $E \leq E_{\gamma}$, which are resonantly coupled with the bulk photon modes, are marked by the bold solid curve. The following parameters relevant to GaAs QWs are used in the numerical calculations: $v_s = 3.7 \times 10^5 \text{ cm s}^{-1}$ and $M_x = 0.3 m_0$ (m_0 is the free electron mass), so that $p_0 \simeq 1.92 \times 10^5 \text{ cm}^{-1}$ and $E_0 \simeq 46.7 \text{ } \mu\text{eV}$ ($E_0/k_B \simeq 0.54 \text{ K}$); $\varepsilon_b = 12.9$ and $\hbar\omega_x(p_{\parallel} = 0) = \hbar\omega_t = 1.55 \text{ eV}$, so that $k_0 \simeq 2.82 \times 10^5 \text{ cm}^{-1}$ and $E_{\gamma} \simeq 101 \text{ } \mu\text{eV}$ ($E_{\gamma}/k_B \simeq 1.17 \text{ K}$).

(iii) to propose and analyse an evaporative optical heating/cooling mechanism for QW excitons.

The underlying physical picture we use refers to the relaxation thermodynamics [11] and assumes a hierarchy of interactions, i.e. that the QW exciton—QW exciton scattering is more efficient than the interaction of QW excitons with bulk LA-phonons. This means that thermalization of QW excitons occurs through the quasi-equilibrium thermodynamic states, which are completely characterized by the effective exciton temperature T and concentration n_{2d} (or degeneracy temperature T_0). The relaxation thermodynamics of indirect excitons deals with $10^9 \text{ cm}^{-2} \leq n_{2d} \leq 10^{11} \text{ cm}^{-2}$ [11]. These concentrations are relevant to the optical experiments [2, 3].

Apart from the bath temperature T_b , there are four control energy parameters in the thermalization and PL dynamics of indirect excitons: $k_B T$, $k_B T_0 \propto n_{2d}$, E_0 and E_{γ} (see figure 1). Bulk LA-phonons couple the ground-state mode $\mathbf{p}_{\parallel} = 0$ with the exciton energy states $E \geq E_0 = \hbar v_s p_0 = 2M_x v_s^2$, i.e. with the exciton energy states which are located inside the LA-phonon dispersion cone. Here v_s is the longitudinal sound velocity. Only low-energy indirect excitons, $0 \leq E \leq E_{\gamma}$, from the radiative zone $|\mathbf{p}_{\parallel}| \leq k_0$ can decay resonantly into the bulk photon modes. The photon wavevector k_0 is given by $k_0 = (\omega_t \sqrt{\varepsilon_b})/c$, where ε_b is the background dielectric constant (see also the caption of figure 1).

In section 2 we discuss LA-phonon-assisted relaxation thermodynamics of indirect excitons for low bath temperatures, $k_B T \leq E_0$. Both classical and quantum mechanisms of slowing down of the thermalization processes are discussed. In section 3 the resonant optical decay of low-energy indirect excitons is considered with detailed analysis of the radiative decay of ultra-cold particles, when $k_B T \leq E_{\gamma}$ and/or $T \leq T_0$. By analysing the quantum diffusion equation, in section 4 we demonstrate an effective screening of interface long-range-correlated QW disorder, i.e. the narrowing effect, by dipole–dipole interacting indirect excitons. In section 5 the PL-jump effect is modelled and attributed to the combination of nearly classical cooling of indirect excitons after the pump pulse and the narrowing effect. In section 6

the evaporative optical heating/cooling processes are analysed for indirect excitons in GaAs coupled QWs. Finally section 7 summarizes our conclusions.

2. Relaxation thermodynamics of QW excitons at low temperatures

The relaxation thermodynamics of QW excitons is given by [11]

$$\frac{\partial}{\partial t} T = -\frac{2\pi}{\tau_{sc}} \left(\frac{T^2}{T_0} \right) (1 - e^{-T_0/T}) \int_1^\infty d\varepsilon \varepsilon \sqrt{\frac{\varepsilon}{\varepsilon-1}} \left| F_z \left(a \sqrt{\varepsilon(\varepsilon-1)} \right) \right|^2 \times \frac{e^{\varepsilon E_0/k_B T_b} - e^{\varepsilon E_0/k_B T}}{(e^{\varepsilon E_0/k_B T} + e^{-T_0/T} - 1)} \frac{1}{(e^{\varepsilon E_0/k_B T_b} - 1)}, \quad (4)$$

where $\tau_{sc} = (\pi^2 \hbar^4 \rho) / (D_{dp}^2 M_x^3 v_s)$ is the characteristic scattering time, ρ is the crystal density and D_{dp} is the deformation potential of exciton-LA-phonon interaction. The form-factor $F_z(\chi) = [\sin(\chi)/\chi][e^{i\chi}/(1 - \chi^2/\pi^2)]$ refers to an infinite rectangular QW confinement potential. This function describes the relaxation of the momentum conservation law in the z -direction (the QW growth direction) and characterizes a spectral band of bulk LA-phonons, which effectively interact with QW excitons. The dimensionless parameter $a \sim 1$ is given by $a = (d_z M_x v_s) / \hbar$, where d_z is the QW thickness.

Equation (4) describes the thermalization dynamics, $T = T(t)$, of QW excitons from the initial effective temperature $T_i = T(t=0)$ to the bath temperature T_b , under the assumption that the total number of particles is conserved. For a classical gas of QW excitons, when T and T_b are much higher than the degeneracy temperature T_0 , equation (4) gives a thermalization time τ_{th}^{cl} of 2–3 orders of magnitude less than that in bulk GaAs. The effective cooling of QW excitons in the presence of a bath of bulk thermal phonons is due to the relaxation of momentum conservation in the z -direction (see the form-factor F_z on the right-hand side of equation (4)): the ground-state mode $\mathbf{p}_{\parallel} = 0$ of QW excitons couples to the continuum exciton states $E \geq E_0$ rather than to the single energy state $E = E_0$ as occurs in bulk materials. For $k_B T_b \gg E_0$, the thermalization time τ_{th}^{cl} is in a few picoseconds timescale, and works in favour of the effective population of the low-energy exciton states. However, at low bath temperatures $k_B T_b \leq E_0$, τ_{th}^{cl} increases exponentially with decreasing T_b , i.e. $\tau_{th}^{cl} \propto \exp(E_0/k_B T_b)$. This effect of classical slowing down of the relaxation kinetics is due to the exponentially small occupation of the exciton states $E \geq E_0$, which can populate the ground-state mode by LA-phonon-assisted Stokes scattering (excitons with energies $E \leq E_0/4$ cannot emit LA-phonons at all). For well-developed Bose–Einstein statistics, when $T \leq T_0$, equation (4) yields quantum slowing down of the thermalization process, so that $\tau_{th}^q \simeq (T_0/T) \tau_{th}^{cl}$ [11].

Linearization of the thermodynamic equation (4), which deals with the described above exponential thermalization, $T = T_b + (T_i - T_b)e^{-t/\tau_{th}}$, does not hold when $|T - T_b|/T_b \geq k_B T_b/E_0$ and, in particular, for $T_b = 0$. For zero bath temperature equation (4) reduces to

$$\frac{\partial}{\partial t} T = -\frac{2\pi}{\tau_{sc}} \left(\frac{T^2}{T_0} \right) (1 - e^{-T_0/T}) \int_1^\infty d\varepsilon \varepsilon \sqrt{\frac{\varepsilon}{\varepsilon-1}} \frac{|F_z(a\sqrt{\varepsilon(\varepsilon-1)})|^2}{e^{\varepsilon E_0/k_B T} + e^{-T_0/T} - 1}. \quad (5)$$

Equation (5), which describes how QW excitons cool down towards $T_b = 0$, can further be simplified for $k_B T$ less than E_0 and $k_B T_0$. In this case one gets

$$\frac{\partial}{\partial t} T = -\frac{2\pi^{3/2}}{\tau_{sc}} \left(\frac{T^2}{T_0} \right) \left(\frac{k_B T}{E_0} \right)^{1/2} e^{-E_0/k_B T}. \quad (6)$$

The right-hand side of equation (6) is proportional to $e^{-E_0/k_B T}$ (classical slowing down) and inversely proportional to T_0 (quantum slowing down). In the dimensionless variables, temperature $\tilde{T} = k_B T/E_0$ and time $\tau = (2\pi^{3/2} E_0 t) / (k_B T_0 \tau_{sc})$, equation (6) reads as

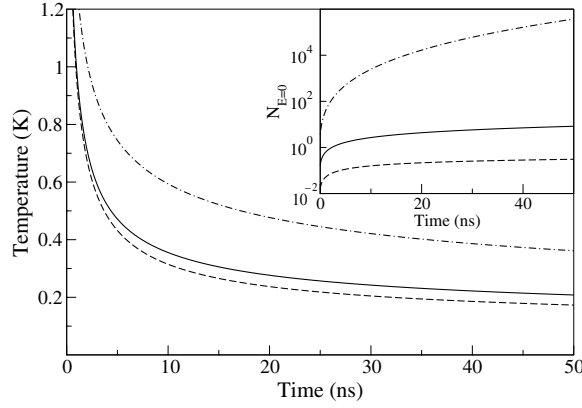


Figure 2. Thermalization dynamics, $T = T(t)$, of QW excitons at $T_b = 0$ K. The initial exciton temperature $T_i = T(t = 0) = 3$ K; $n_{2d} = 10^9$ cm $^{-2}$ (dashed curve), 10^{10} cm $^{-2}$ (solid curve) and 10^{11} cm $^{-2}$ (dash-dotted curve). The degeneracy temperature $T_0 \propto n_{2d}$ is equal to 0.46 K for $n_{2d} = 10^{10}$ cm $^{-2}$. In addition to the GaAs parameters listed in the caption of figure 1, we use $d_z = 8$ nm, $D_{dp} = 8.2$ eV and $\rho = 5.3$ g cm $^{-3}$. Inset: population dynamics of the ground-state mode, $N_{E=0} = N_{E=0}(t)$.

$d\tilde{T}/d\tau = -\tilde{T}^{5/2}e^{-1/\tilde{T}}$. Thus, the solution $T = T(t)$ of equation (6) is given by the transcendental equation:

$$F(\tilde{T} = k_B T/E_0) = \tau + C_i = \frac{2\pi^{3/2}}{\tau_{sc}} \left(\frac{E_0}{k_B T_0} \right) t + C_i, \quad (7)$$

where $F(x) = [1/\sqrt{x} - \text{Ds}(1/\sqrt{x})]e^{1/x}$ and $\text{Ds}(y) = e^{-y^2} \int_0^y dt e^{t^2}$ is Dawson's integral. The integration constant C_i is determined by the initial condition $T_i = T(t = 0) \leq E_0/k_B$, i.e. $C_i = F(k_B T_i/E_0)$.

According to equation (7), for $t \gg [(k_B T_0)/(2\pi^{3/2} E_0)]\tau_{sc}$ the asymptotic solution of equation (6) is

$$k_B T(t) = \frac{E_0}{\ln[(2\pi^{3/2} E_0 t)/(k_B T_0 \tau_{sc})]}, \quad (8)$$

i.e. $\tilde{T}(\tau) = 1/\ln(\tau)$ for $\tau \gg 1$. Both factors, classical and quantum slowing down of the relaxation kinetics, together with the need to accumulate a huge number of QW excitons in the ground-state mode $\mathbf{p}_{\parallel} = 0$, due to BE statistics, are responsible for the nonexponential and extremely slow thermalization law $1/\ln(\tau)$ for $T_b = 0$. The corresponding occupation kinetics of the ground-state mode for $\tau \gg 1$ is given by

$$N_{E=0}(\tau) = \tau^{k_B T_0/E_0}. \quad (9)$$

The nonexponential population law (9) of the ground-state mode $E = 0$ is similar to that found for thermalization of excitons in bulk semiconductors at $T \leq T_c$ [12, 13]. Equation (9) is also consistent with a generic solution of the LA-phonon-assisted relaxation kinetics of QW excitons at low densities ($n_{2d} \leq 10^9$ cm $^{-2}$ for GaAs QWs) [14].

The results of numerical simulations of the thermalization dynamics at $T_b = 0$, calculated with equation (5), are plotted in figure 2 for $n_{2d} = 10^9$, 10^{10} and 10^{11} cm $^{-2}$, and for the same initial effective temperature $T_i = 3$ K. After the first transient relaxation of relatively hot QW excitons, which lasts a few nanoseconds, the thermalization dynamics reveals the density-dependent $T \sim 1/\ln(t)$ law given by equation (8). According to equation (9), the power-law population dynamics of the ground-state mode $\mathbf{p}_{\parallel} = 0$ becomes particularly effective for $k_B T_0 > E_0$ (see the inset of figure 2), i.e. in the high-density limit.

At very large delay times the thermalization law becomes $1/t$ [15], and starts to dominate over the $1/\ln(t)$ relaxation dynamics described above. The $1/t$ thermalization law is due to the exciton–exciton scattering processes, which are treated beyond the relaxation thermodynamics used in our study. Furthermore, the $1/\ln(t)$ (and later on, $1/t$) thermalization dynamics cannot be completely realized in GaAs coupled quantum wells, due to the continuous optical decay of low-energy QW excitons. The latter usually deals with a 10 ns timescale [7, 8]. For the same reason, as we demonstrate below, the occupation numbers $N_{E=0} > 100\text{--}200$ are highly unlikely to occur. There is also no need to keep the cryostat temperature at extremely low $T_b = 50$ mK, because within the optical lifetime of QW excitons, τ_{opt} , the effective exciton temperature T is far above 0.1 K (see figure 2). For example, for $n_{2d} = 10^{11}$ cm $^{-2}$ one has $T(t = 10$ ns) $\simeq 0.59$ K.

3. Optical decay of statistically-degenerate QW excitons

In high-quality QWs a quasi-2D exciton can emit a bulk photon only from the low-energy, radiative modes, which are located inside the photon cone $k = k(\omega) = (\sqrt{\epsilon_b}\omega)/c$ (ω is the frequency of the light field). Thus the radiative zone of QW excitons is given by $p_{\parallel} \leq k_0$, where $k_0 = k(\omega_t)$ corresponds to the crossover point between the photon and exciton dispersions (see figure 1). Similar to the thermalization kinetics, the optical evaporation of QW excitons is also sensitive to Bose–Einstein statistics of the low-energy radiative states [11]. The effective radiative decay rate of BE-distributed QW excitons, Γ_{opt} , is given by

$$\Gamma_{\text{opt}} \equiv \frac{1}{\tau_{\text{opt}}} = \frac{1}{2\tau_{\text{R}}} \left(\frac{E_{\gamma}}{k_{\text{B}}T_0} \right) \int_0^1 \frac{1+z^2}{Ae^{-z^2E_{\gamma}/k_{\text{B}}T} - 1} dz, \quad (10)$$

where

$$A = A(T, T_0) = \frac{e^{E_{\gamma}/k_{\text{B}}T}}{1 - e^{-T_0/T}}, \quad (11)$$

and τ_{R} is the intrinsic radiative lifetime of ground-state QW excitons with in-plane momentum $\hbar\mathbf{p}_{\parallel} = 0$. Equation (10) takes into account the equal probabilities of the in-plane T- and L-polarizations of optically-active QW excitons (or, in other words, the equal populations of the σ^+ - and σ^- -polarized QW exciton states). The two-fold optically-inactive, ‘dark’ QW exciton states are included in equation (10) through the degeneracy temperature T_0 , which is proportional to the total concentration n_{2d} of QW excitons.

For the high-temperature limit, when $k_{\text{B}}T$ is much larger than $k_{\text{B}}T_0$ and E_{γ} , the QW excitons are Maxwell–Boltzmann distributed (see equation (2)), and equation (10) yields the effective radiative lifetime $\tau_{\text{opt}}^{\text{cl}}$:

$$\tau_{\text{opt}}^{\text{cl}} = \left(\frac{3k_{\text{B}}T}{2E_{\gamma}} \right) \tau_{\text{R}} + \left(\frac{9}{10} - \frac{3k_{\text{B}}T_0}{4E_{\gamma}} \right) \tau_{\text{R}}. \quad (12)$$

The first, leading term on the right-hand side of equation (12) is the well-known estimate of the optical lifetime, $\tau_{\text{opt}} = \tau_{\text{opt}}^{\text{cl}(0)} = (3k_{\text{B}}T\tau_{\text{R}})/(2E_{\gamma})$, in the limit of well-developed classical statistics of QW excitons. The optical lifetime $\tau_{\text{opt}}^{\text{cl}(0)}$ is much larger than the intrinsic radiative lifetime τ_{R} , because for $T \gg T_0$, E_{γ}/k_{B} only a small fraction of QW excitons occupy the radiative modes $p_{\parallel} \leq k_0$. The temperature-independent correction to $\tau_{\text{opt}}^{\text{cl}}$, given by the second term on the right-hand side of equation (12), consists of the concentration-independent and concentration-dependent contributions of opposite signs. The concentration-dependent contribution, which is proportional to the degeneracy temperature T_0 , originates from BE statistics of QW excitons. Thus the influence of nonclassical statistics can be traced in the photoluminescence of QW excitons even for high temperatures.

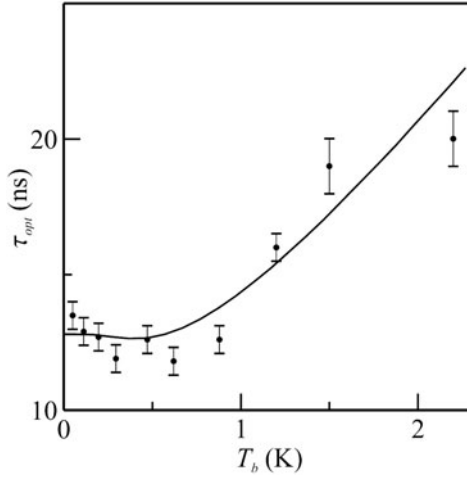


Figure 3. The optical decay time of excitons in GaAs coupled QWs, τ_{opt} , against the cryostat (bath) temperature T_b : numerical evaluation of equation (10) (solid curve) and experimental data (circles with error bars). The intrinsic radiative lifetime of QW excitons is given by $\tau_R = 6.75$ ns. The density of QW excitons, $n_{2d} = 2 \times 10^{10} \text{ cm}^{-2}$, used in the numerical calculations, is relevant to the pump intensities used in the experiments [2, 3]. From [16].

For strongly statistically-degenerate quasi-2D excitons, when $T \ll T_0$, equation (10) yields the quantum limit of Γ_{opt} :

$$\Gamma_{\text{opt}}^q = \left[1 - \frac{T}{T_0} + \frac{T}{T_0} \ln \left(\frac{4E_\gamma}{k_B T} \right) \right] \frac{\Gamma_0}{2}, \quad (13)$$

where $\Gamma_0 = 1/\tau_R$. The second and third terms in the square brackets on the right-hand side of equation (13) are small temperature-dependent corrections, i.e. $\Gamma_{\text{opt}}^q(T \rightarrow 0) \rightarrow \Gamma_0/2$. An accumulation of QW excitons with occupation numbers $N_E \gg 1$ in close vicinity of the ground-state mode $\mathbf{p}_\parallel = 0$ gives rise to the above limit. Thus, the optical decay time of highly-degenerate QW excitons is given by $\tau_{\text{opt}}^q(T \rightarrow 0) \rightarrow 2\tau_R$. The factor 2 in the above expressions for Γ_{opt}^q and τ_{opt}^q is due to the optically-inactive QW excitons. For $T \leq E_\gamma/k_B \simeq 1$ K (for GaAs QWs with no magnetic field applied to the structure), the effective radiative lifetime τ_{opt} approaches $2\tau_R$ nearly independently of the degree of quantum degeneracy.

Figure 3 shows the comparison of τ_{opt} , calculated with equation (10), and the optical lifetime of indirect excitons in GaAs coupled QWs, measured at very low cryostat temperatures, $50 \text{ mK} \leq T_b \leq 2 \text{ K}$ [16]. The calculated dependence $\tau_{\text{opt}} = \tau_{\text{opt}}(T_b)$ does reproduce in detail the measured values of τ_{opt} . In particular, $\tau_{\text{opt}} \simeq 2\tau_R$ for $T_b \leq E_\gamma/k_B \simeq 1$ K and $\tau_{\text{opt}} \propto T_b$ for $T_b > 1$ K, according to equation (12). Even a local minimum of $\tau_{\text{opt}}(T_b)$, described by equation (13) for statistically-degenerate QW excitons, has been observed at low cryostat temperature $T_b \simeq 0.5$ K (see figure 3). In the numerical evaluations of equation (10) we assume $T = T_b$ and $n_{2d} = 2 \times 10^{10} \text{ cm}^{-2}$. The only critical fit parameter used in the calculations is the intrinsic radiative lifetime: $\tau_R = 6.75$ ns. In fact the experiments with low $T_b \leq E_\gamma/k_B$ allow us to measure the intrinsic radiative lifetime τ_R of indirect excitons.

4. Screening of the QW interface disorder by indirect excitons

The inhomogeneous linewidth of the PL signal associated with the resonant optical decay of indirect excitons in high-quality GaAs/AlGaAs coupled QWs, $\hbar\Gamma_{\text{inhom}} \simeq 0.7\text{--}1$ meV [2, 3], is still much larger than the homogeneous linewidth $\hbar\Gamma_{\text{hom}} = E_\gamma \simeq 0.1$ meV. The above values of Γ_{inhom} and Γ_{hom} are relevant to indirect excitons at low, helium bath temperatures T_b and low concentrations $n_{2d} \leq 10^9 \text{ cm}^{-2}$. Because $\hbar\Gamma_{\text{inhom}}$ is larger than the control parameters of the model, E_0 and E_γ , a natural question arises as to what extent our theory is adequate to

explain the experimental results. In this section we discuss the narrowing effect—an effective screening of QW disorder by dipole–dipole interacting indirect excitons. The in-plane diffusion of indirect excitons in the presence of a spatially-fluctuating QW potential gives rise to the screening effect. A quantum diffusion equation, analysed below, describes the narrowing effect for long-range-correlated disorder.

The nonlinear quantum diffusion equation for indirect excitons in (GaAs) coupled QWs is given by [10]

$$\frac{\partial n_{2d}}{\partial t} = \nabla \left[D_x^{(2d)} \nabla n_{2d} + \frac{2}{\pi} \left(\frac{M_x}{\hbar^2} \right) (e^{T_0/T} - 1) D_x^{(2d)} \nabla (u_0 n_{2d} + U_{QW}) \right] - \Gamma_{\text{opt}} n_{2d} + \Lambda, \quad (14)$$

where $\Gamma_{\text{opt}} = 1/\tau_{\text{opt}}$ is given by equation (10), $D_x^{(2d)} = D_x^{(2d)}(T, T_0)$ is the diffusion coefficient of QW excitons, Λ is the generation rate of excitons, U_{QW} is the in-plane QW potential, and the operator ∇ is defined in terms of the in-plane coordinate, $\mathbf{r}_{\parallel} = \{x, y\}$. The in-plane random potential $U_{QW} = U_{\text{rand}}(\mathbf{r}_{\parallel})$ is due to the QW thickness and alloy fluctuations. The drift motion of QW excitons is proportional to ∇U_{eff} , where $U_{\text{eff}} = u_0 n_{2d} + U_{QW}$ (see the last term in the square brackets on the right-hand side of equation (14)). The mean-field energy, $U_{\text{mf}} = u_0 n_{2d}$, is due to the well-defined dipole–dipole repulsive interaction of indirect excitons (the indirect excitons can be interpreted as an in-plane ensemble of identical dipoles oriented normal to the QW structure). The potential u_0 is not sensitive to the internal spin structure of indirect excitons and is given by $u_0 = (2\pi\hbar^2 d_z)/(\mu_x a_x^{(2d)}) = 4\pi(e^2/\varepsilon_b)d_z$. Here μ_x and $a_x^{(2d)} = (\hbar^2 \varepsilon_b)/(2\mu_x e^2)$ are the in-plane reduced mass and Bohr radius of excitons, respectively. It is the mean-field interaction energy $u_0 n_{2d}$ that is responsible for the screening effect. The underlying physical picture is that the QW excitons tend to accumulate near the minima of $U_{\text{rand}}(\mathbf{r}_{\parallel})$ (local increase of $u_0 n_{2d}(\mathbf{r}_{\parallel})$) and to avoid the maxima of $U_{\text{rand}}(\mathbf{r}_{\parallel})$ (local decrease of $u_0 n_{2d}(\mathbf{r}_{\parallel})$). Note that for the GaAs coupled QW structures, used in the experiments [2, 3], one estimates $U_{\text{mf}}^{(0)} = u_0 n_{2d}^{(0)} \simeq 1.4\text{--}1.6$ meV for $n_{2d}^{(0)} = 10^{10}$ cm⁻².

In order to analyse the narrowing effect analytically, we put $\Gamma_{\text{opt}} = 0$ (no optical decay of excitons) and $\Lambda = 0$ (no source of excitons). In this case, a steady-state solution n_{2d} of equation (14) yields for average concentrations such that $n_{2d}^{(0)} \gg |U_{\text{rand}}(\mathbf{r}_{\parallel})|/u_0$:

$$U_{\text{eff}} = u_0 n_{2d}^{(0)} + \frac{U_{\text{rand}}(\mathbf{r}_{\parallel})}{1 + [(2M_x)/(\pi\hbar^2)](e^{T_0/T} - 1)u_0}, \quad (15)$$

where $U_{\text{eff}} = U_{\text{rand}}(\mathbf{r}_{\parallel}) + u_0 n_{2d}(\mathbf{r}_{\parallel})$ is the effective, screened in-plane potential. The narrowing effect for the long-range-correlated random potential is described by the second term on the right-hand side of equation (15). For $u_0 n_{2d}^{(0)} \gg |U_{\text{rand}}|$ the denominator of the second term is much larger than unity. In particular, for classical statistics, when $T \gg T_0$, equations (14) and (15) yield

$$n_{2d}(\mathbf{r}_{\parallel}) = n_{2d}^{(0)} - \frac{U_{\text{rand}}(\mathbf{r}_{\parallel})n_{2d}^{(0)}}{k_B T + u_0 n_{2d}^{(0)}}, \quad U_{\text{eff}}(\mathbf{r}_{\parallel}) = u_0 n_{2d}^{(0)} + \frac{U_{\text{rand}}(\mathbf{r}_{\parallel})k_B T}{k_B T + u_0 n_{2d}^{(0)}}. \quad (16)$$

For $u_0 n_{2d}^{(0)} \gg k_B T$, equation (16) describes strong suppression of the potential fluctuations: $U_{\text{rand}}(\mathbf{r}_{\parallel}) \rightarrow \kappa U_{\text{rand}}(\mathbf{r}_{\parallel})$, where $\kappa = (k_B T)/(u_0 n_{2d}^{(0)}) \ll 1$. Due to the exponential function $\exp(T_0/T)$ on the right-hand side of equation (15), the screening effect becomes particularly strong in the quantum regime, when $T_0 \geq T$. Figure 4 shows the effective potential $U_{\text{eff}}(x)$ and concentration of excitons $n_{2d}(x)$, calculated with equation (14) for a model one-dimensional long-range-correlated random potential $U_{\text{rand}}(x)$ (bold solid curves in figure 4), and realistic values of $n_{2d}^{(0)}$, $D_x^{(2d)}$, T , τ_{opt} and $|U_{\text{rand}}| \sim 0.5$ meV. According to figure 4, for the average density $n_{2d}^{(0)} \simeq 10^{10}$ cm⁻² and exciton temperature $T \sim 1$ K the long-range-correlated in-plane disorder is already drastically screened and relaxed.

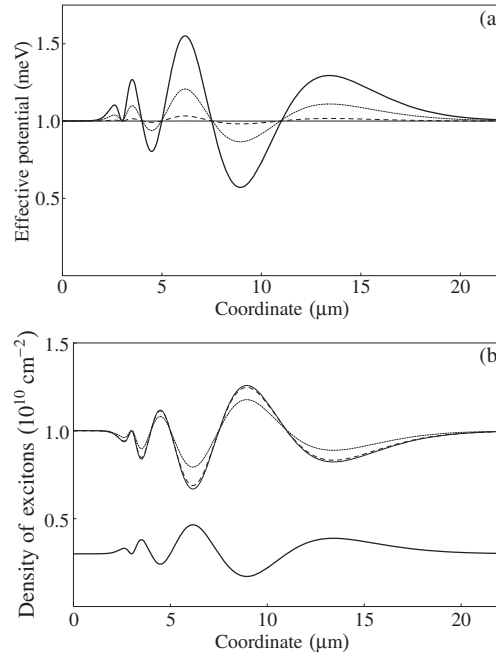


Figure 4. Temperature dependence of the narrowing effect, due to screening of long-range-correlated disorder by dipole–dipole interacting indirect excitons in GaAs coupled QWs. The diffusion coefficient $D_x^{(2d)} = 100 \text{ cm}^2 \text{ s}^{-1}$, the optical lifetime $\tau_{\text{opt}} = 20 \text{ ns}$ and the generation rate $\Lambda = 5 \times 10^8 \text{ cm}^{-2} \text{ ns}^{-1}$, so that the average concentration of indirect excitons $n_{2d}^{(0)} \simeq 10^{10} \text{ cm}^{-2}$. (a) The effective potential $U_{\text{eff}}(x) = U_{\text{rand}}(x) + u_0 n_{2d}(x)$ and (b) local concentration $n_{2d}(x)$ against the in-plane coordinate x . The exciton temperature is $T = 10 \text{ K}$ (dotted curves), 1 K (dashed curves) and 0.1 K (thin solid curves). In both figures the input, unscreened potential $U_{\text{rand}}(x)$ is shown by bold solid curves (note that in the upper figure U_{rand} is shifted by $+1 \text{ meV}$ and U_{eff} is shifted by $-u_0 n_{2d}^{(0)} + 1 \text{ meV} \simeq -0.66 \text{ meV}$, and in the lower figure U_{rand} is plotted in au). The n_{2d} -dependence of the screening effect is shown in figure 2 of [10].

The mean-field potential $U_{\text{mf}} = u_0 n_{2d}$ also gives rise to the narrowing effect for mid-range-correlated in-plane disorder (length scale of a few $a_x^{(2d)}$). In this case the dipole–dipole repulsive interaction considerably decreases the localization energy of indirect excitons in a mesoscopic in-plane trap. Short-range 2D disorder, which can be described in terms of a random contact potential, is also strongly suppressed by interacting bosons [17]. Thus we conclude that in high-quality GaAs-based coupled QWs the in-plane random potential $U_{\text{QW}} = U_{\text{rand}}$ of any correlation length is effectively screened and practically removed at $n_{2d}^{(0)} \geq 10^{10} \text{ cm}^{-2}$, due to the dipole–dipole repulsive interaction of indirect excitons. In this case the in-plane momentum $\hbar \mathbf{p}_{\parallel}$ becomes a good quantum number even for very low-energy indirect excitons. Thus the phonon-assisted relaxation and photoluminescence kinetics, which we study in this paper in terms of well-defined \mathbf{p}_{\parallel} , are adequate for explanation and modelling of the experiments on statistically-degenerate excitons in GaAs/AlGaAs coupled QWs [2, 3].

5. The PL-jump: origin and modelling

The relaxation and PL dynamics of photogenerated indirect excitons are given by

$$\frac{\partial}{\partial t} n_{2d} = -\frac{n_{2d}}{\tau_{\text{opt}}} + \Lambda(t), \quad \frac{\partial}{\partial t} T = \left(\frac{\partial T}{\partial t} \right)_{n_{2d}} + S_T(t), \quad (17)$$

where $\tau_{\text{opt}} = \tau_{\text{opt}}(T, T_0) = 1/\Gamma_{\text{opt}}$ is given by equation (10), $\Lambda(t)$ is the generation rate of indirect excitons by an optical pulse, and $(\partial T/\partial t)_{n_{2d}}$ is given by the right-hand side of equation (4). The term S_T , which describes the change of T due to the nonresonant optical pump and resonant radiative decay of indirect excitons, is

$$S_T = \frac{(E_{\text{inc}} - k_B T I_2 \tilde{A}) \Lambda_{T_0} - [E_\gamma/\tau_{\text{opt}}^E - (k_B T I_2 \tilde{A})/\tau_{\text{opt}}] T_0}{2k_B T I_1 - k_B T_0 I_2 \tilde{A}}, \quad (18)$$

where $\tilde{A} = \tilde{A}(T, T_0) = e^{-T_0/T}/(1 - e^{-T_0/T})^2$, $\Lambda_{T_0} = [(\pi \hbar^2)/(2M_x)]\Lambda(t)$ and the integrals $I_{1,2} = I_{1,2}(T, T_0)$ are given by

$$\begin{aligned} I_1 &= (1 - e^{-T_0/T}) \int_0^\infty \frac{z \, dz}{e^z + e^{-T_0/T} - 1}, \\ I_2 &= (1 - e^{-T_0/T})^2 \int_0^\infty \frac{z e^z \, dz}{(e^z + e^{-T_0/T} - 1)^2}. \end{aligned} \quad (19)$$

The characteristic time τ_{opt}^E of the energy relaxation, due to the resonant optical decay of QW excitons, is determined by

$$\frac{1}{\tau_{\text{opt}}^E} = \frac{1}{2\tau_R} \left(\frac{E_\gamma}{k_B T_0} \right) \int_0^1 \frac{1 - z^4}{A e^{-z^2 E_\gamma/k_B T} - 1} \, dz, \quad (20)$$

where A is given by equation (11).

The experiments [2, 3] deal with an in-plane large area of the GaAs coupled QWs homogeneously excited by a rectangular optical pulse of about 50 ns duration. The optical excitation is nonresonant, i.e. the pump photon energy $\hbar\omega_{\text{pulse}} \simeq 1.85$ eV is much larger than the indirect QW exciton energy $\hbar\omega_t \simeq 1.54$ – 1.56 eV. Thus the photogeneration of indirect excitons is a secondary process, due either to quantum tunnelling of direct QW excitons into the energetically more favourable states of indirect excitons, or to a resonant Coulomb binding of initially photogenerated electrons and holes after they complete an LO-phonon cascade emission. In both cases the excess energy of created (incoming), hot indirect excitons is large, $E_{\text{inc}} \simeq 10$ – 30 meV. In equations (17) and (18) we assume a monoenergetic injection of indirect excitons. A contribution to S_T (see equation (18)), which is proportional to E_{inc} , has positive sign and describes a heating process by incoming, hot indirect excitons. The rest of S_T can either be positive or negative and deals with heating or cooling, due to the resonant optical evaporation of indirect excitons.

In figure 5 we plot the resonant PL signal from indirect excitons, calculated with equations (17) for $T_b = 0.05$ K and a rectangular excitation pulse of $\tau_{\text{pulse}} = 47$ ns. The parameters used in the calculations correspond to those relevant to the optical experiments [2, 3]. The generation rate $\Lambda = 1.3 \times 10^9 \text{ cm}^{-2} \text{ ns}^{-1}$ (solid curve in figure 5) gives at the end of the excitation pulse the maximum density $n_{2d}^{\text{max}} \simeq 2.9 \times 10^{10} \text{ cm}^{-2}$. The latter value reproduces n_{2d}^{max} generated by using a maximum laser intensity: in the experiments, n_{2d}^{max} can be estimated by attributing a blue shift of the PL line to the mean-field energy $U_{\text{mf}} = u_0 n_{2d}$. A still further increase of the pump rate, in the numerical modelling with equations (17), to $\Lambda = 4.8 \times 10^9 \text{ cm}^{-2} \text{ ns}^{-1}$ (dash-dotted curve in figure 5) yields $n_{2d}^{\text{max}} \simeq 9.5 \times 10^{10} \text{ cm}^{-2}$. The PL-jump, observed in the experiments [2, 3], is clearly seen in the calculated PL dynamics, $I_{\text{PL}} = I_{\text{PL}}(t)$, plotted in figure 5. In figure 6 we show the time dependence of n_{2d} , τ_{opt} , $N_{E=0}$ and T , modelled with equations (10), (17)–(20) for $T_b = 0.05$ K and $\Lambda = 1.3 \times 10^9 \text{ cm}^{-2} \text{ ns}^{-1}$. The solid (dashed) curves refer to $H_\perp = 0$ ($H_\perp = 14$ T). A strong magnetic field of $H_\perp = 14$ T, applied perpendicularly to the GaAs QW structure, increases the in-plane mass of indirect excitons to $M_x(H_\perp = 14 \text{ T}) \simeq 7.1 M_x \simeq 2.1 m_0$, according to the estimate done by using

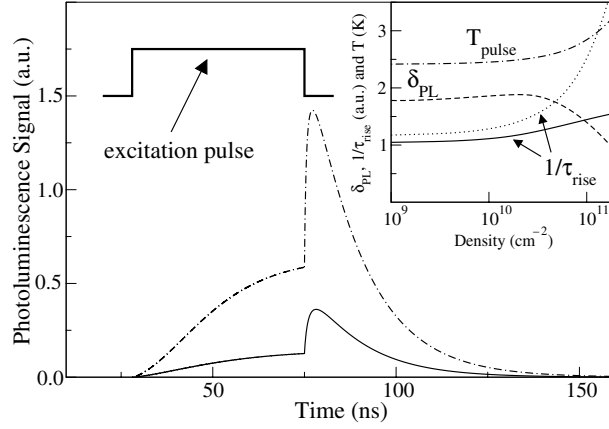


Figure 5. Resonant photoluminescence of indirect excitons against time t . I_{PL} is calculated from low-energy QW excitons with $|\mathbf{p}_{\parallel}| \leq p_{\parallel}^{\text{PL}} \simeq 0.77k_0$. The rectangular excitation pulse of duration $\tau_{\text{pulse}} = 47$ ns starts at $t_0 = 28$ ns. The bath temperature $T_b = 50$ mK, the intrinsic radiative lifetime $\tau_R = 6.75$ ns, the energy of hot (incoming) photogenerated excitons $E_{\text{inc}} = 17.2$ meV ($E_{\text{inc}}/k_B = 200$ K) and the other parameters of the GaAs coupled QW are the same as for figure 2. The pump rate $\Lambda = 1.3 \times 10^9$ cm $^{-2}$ ns $^{-1}$ (solid curve) yields $n_{2d}^{\text{max}} = 2.87 \times 10^{10}$ cm $^{-2}$, and $\Lambda = 4.8 \times 10^9$ cm $^{-2}$ ns $^{-1}$ (dash-dotted curve) gives $n_{2d}^{\text{max}} = 9.51 \times 10^{10}$ cm $^{-2}$. Inset: the effective temperature of indirect excitons at the end of the excitation pulse, $T_{\text{pulse}} = T(t = t_0 + \tau_{\text{pulse}})$ (dash-dotted curve), the rise rate of the PL signal, $1/\tau_{\text{rise}} = [d \ln(I_{\text{PL}})/dt]_{t=t_0+\tau_{\text{pulse}}}$ (solid curve), and the PL jump contrast, $\delta_{\text{PL}} = \Delta I_{\text{PL}}/I_{\text{PL}}$, against $n_{2d}^{\text{max}} = n_{2d}(t = t_0 + \tau_{\text{pulse}})$. The rise rate $1/\tau_{\text{rise}}$ calculated for $p_{\parallel}^{\text{PL}} \rightarrow 0$ is shown by the dotted curve.

figure 2 of [4]. Apart from the change of M_x , in numerical modelling for $H_{\perp} = 14$ T one uses the spin degeneracy factor $g = 1$ (see equation (1)).

Numerical simulations of the thermalization and PL dynamics allow us to clarify the origin of the PL-jump. At the end of the pump pulse, the exciton temperature $T(t = t_0 + \tau_{\text{pulse}}) = T_{\text{pulse}}$ is still much higher than $T_b = 50$ mK and approaches a steady-state value, if $\tau_{\text{pulse}} \rightarrow \infty$ (see figure 6(d)). The latter value refers to the steady-state concentration, $n_{2d}^{\text{max}}(\tau_{\text{pulse}} \rightarrow \infty) \rightarrow \Lambda \tau_{\text{opt}}$, and is due to a balance between injected and thermalized energies. In other words, incoming, hot indirect excitons effectively heat the excitonic system. In the inset of figure 5, the calculated values of T_{pulse} are plotted against n_{2d}^{max} for $\tau_{\text{pulse}} = 47$ ns: T_{pulse} is about 2.5 K for $n_{2d}^{\text{max}} \leq 5 \times 10^{10}$ cm $^{-2}$ and increases to 2.8 K for $n_{2d}^{\text{max}} = 10^{11}$ cm $^{-2}$. Right after the trailing edge of the excitation pulse, the exciton temperature starts to decrease rapidly from $T = T_{\text{pulse}}$. As a result, the optical lifetime τ_{opt} decreases (see figure 6(b)), due to more efficient population of the low-energy optically-active excitonic states, and gives rise to the rapid increase of I_{PL} , i.e. to the PL-jump. Now we need to realize how strongly BE statistics contribute to this nearly classical scenario.

While all the optically-active low-energy states $|\mathbf{p}_{\parallel}| \leq k_0$ contribute to the total optical decay of QW excitons (see equation (10)), the PL signal is observed in the normal, z -direction within a collection angle 2α . In order to model the PL-jump contrast, $\delta_{\text{PL}} = [I_{\text{PL}}^{\text{max}}(t = t_0 + \tau_{\text{pulse}} + t_{\text{max}}) - I_{\text{PL}}(t = t_0 + \tau_{\text{pulse}})]/I_{\text{PL}}(t = t_0 + \tau_{\text{pulse}})$, observed in the experiments [2, 3], in the numerical evaluations of I_{PL} we assume that the PL signal is collected from the states $|\mathbf{p}_{\parallel}| \leq 0.77k_0$. This corresponds to $\alpha \simeq 50^\circ$ and gives $\delta_{\text{PL}} \simeq 1-2$ (see the inset of figure 5), similar to the observed values of δ_{PL} . Here $t_{\text{max}} \simeq 6-7$ ns is the delay time after the pump pulse, when the maximum PL signal occurs. For the collection angle $2\alpha \rightarrow 0$, when the ground-state occupation number $N_{E=0}$ is directly probed, the PL-jump contrast increases from $\delta_{\text{PL}} \simeq 3$

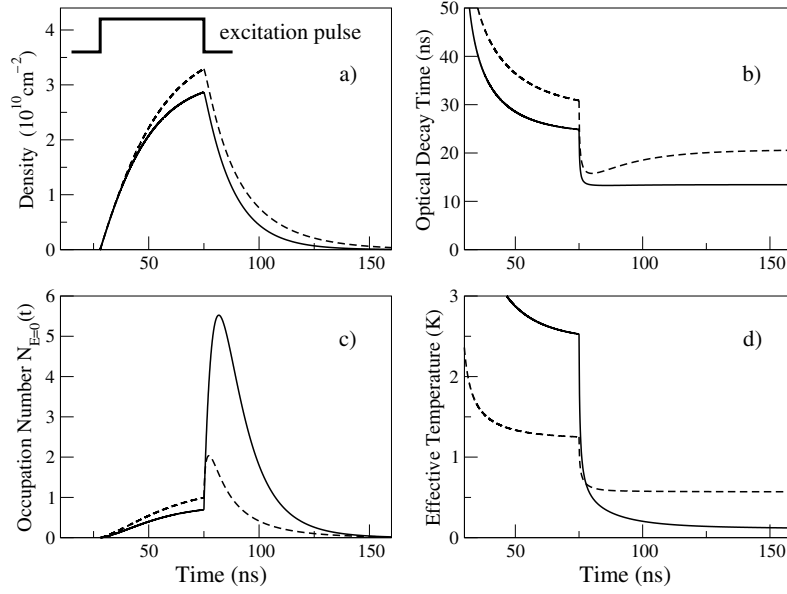


Figure 6. Relaxation and photoluminescence kinetics of indirect excitons calculated with equations (17). The generation rate of indirect excitons by the rectangular pump pulse is $\Lambda = 1.3 \times 10^9 \text{ cm}^{-2} \text{ ns}^{-1}$, and the bath temperature is $T_b = 50 \text{ mK}$. The other characteristics of the excitation pulse and parameters of the GaAs structure are the same as for figure 5. The magnetic field $H_{\perp} = 0$ (solid curves) and $H_{\perp} = 14 \text{ T}$ (dashed curves): (a) $n_{2d} = n_{2d}(t)$, (b) $\tau_{\text{opt}} = \tau_{\text{opt}}(t)$, (c) $N_{E=0} = N_{E=0}(t)$ and (d) $T = T(t)$.

for $n_{2d}^{\text{max}} \simeq 10^9 \text{ cm}^{-2}$ towards $\delta_{\text{PL}} \simeq 7$ for $n_{2d}^{\text{max}} \simeq 3 \times 10^{10} \text{ cm}^{-2}$. The latter values of δ_{PL} are much higher than those detected in the experiments [2, 3]. In [3] the observed nonlinear increase of the PL signal right after the pump pulse is attributed to bosonic stimulation of the scattering of indirect excitons into the highly populated ground-state mode $\mathbf{p}_{\parallel} = 0$. In the inset of figure 5 we plot the rise rate of the PL signal, $1/\tau_{\text{rise}} = [d \ln(I_{\text{PL}})/dt]_{t=t_0+\tau_{\text{pulse}}}$, against n_{2d}^{max} for $\alpha = 50^\circ$ (solid curve) and $\alpha \rightarrow 0$ (dotted curve). The calculations are done with equations (17). According to the plot (see the inset of figure 5), the rise rate $1/\tau_{\text{rise}}$ is nearly independent of n_{2d}^{max} for the values $10^9 \text{ cm}^{-2} \leq n_{2d}^{\text{max}} \leq 3 \times 10^{10} \text{ cm}^{-2}$, which are used in the experiments [2, 3]. With still further increase of n_{2d}^{max} , the nonlinear behaviour starts to develop so that $1/\tau_{\text{rise}}$ increases by a factor 3 (for $\alpha \rightarrow 0$) or 1.4 (for $\alpha = 50^\circ$) for $n_{2d}^{\text{max}} \simeq 1.5 \times 10^{11} \text{ cm}^{-2}$.

Thus we conclude that the observed strongly nonlinear increase of $1/\tau_{\text{rise}}$ with increasing n_{2d}^{max} cannot be explained by bosonic stimulation of the scattering processes into the ground-state mode. The bosonic stimulation effect refers to the ‘explosive’ population of the ground-state mode, when $T \rightarrow 0$ and $k_B T_0/E_0 \gg 1$ (see equation (9)). The above conditions do not hold for $n_{2d}^{\text{max}} \leq 3 \times 10^{10} \text{ cm}^{-2}$. The PL-jump is mainly due to classical cooling of indirect excitons right after the trailing edge of the rectangular excitation pulse. In the presence of the continuous optical decay of indirect excitons, nonclassical population of the low-energy states cannot effectively build up: $N_{E=0}^{\text{max}} \simeq 5.5$ for $n_{2d}^{\text{max}} = 2.87 \times 10^{10} \text{ cm}^{-2}$ and $N_{E=0}^{\text{max}} \simeq 122.7$ for $n_{2d}^{\text{max}} = 9.51 \times 10^{10} \text{ cm}^{-2}$ (see figures 7 and 6(c)). Note that these values of $N_{E=0}^{\text{max}}$ are much less than the typical values of $N_{E=0}(t)$ calculated with equation (4) for $1/\tau_{\text{opt}} = 0$ and nearly identical conditions (see figure 2).

Numerical simulations of the thermalization and photoluminescence dynamics with equations (17) yield a strong decrease of the PL-jump contrast, δ_{PL} , with increasing H_{\perp}

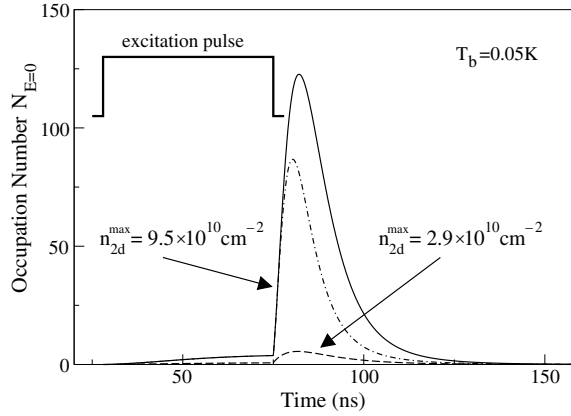


Figure 7. Population dynamics of the ground-state mode, $N_{E=0} = N_{E=0}(t)$, calculated with equations (17) for $n_{2d}^{\max} \simeq 2.87 \times 10^{10} \text{ cm}^{-2}$ ($\Lambda = 1.3 \times 10^9 \text{ cm}^{-2} \text{ ns}^{-1}$, dashed curve) and $n_{2d}^{\max} \simeq 9.51 \times 10^{10} \text{ cm}^{-2}$ ($\Lambda = 4.8 \times 10^9 \text{ cm}^{-2} \text{ ns}^{-1}$, solid curve). The other parameters are the same as for figure 5. For comparison, $N_{E=0} = N_{E=0}(t)$ calculated with no cooling effect due to the optical evaporation (in equations (17) and (18) one puts $S_T = 0$ for $t \geq t_0 + \tau_{\text{pulse}}$) is shown by the dash-dotted curve.

(see figure 6(c)) and/or increasing T_b , in complete agreement with the experimental results [2, 3]. However, the dependence of δ_{PL} upon n_{2d}^{\max} , i.e. upon the pump intensity Λ , is extremely weak for $10^9 \text{ cm}^{-2} \leq n_{2d}^{\max} \leq 3 \times 10^{10} \text{ cm}^{-2}$ (see the inset of figure 5), in sharp contrast with observations [2, 3] of complete disappearance of the PL-jump at $n_{2d}^{\max} \simeq 10^9 \text{ cm}^{-2}$. Note that the persistence of the PL-jump even for very low n_{2d}^{\max} , according to the numerical calculations with equations (17), is another manifestation of the classical character of the PL-jump phenomenon.

Both contradictions between the experimental results and numerical modelling with equations (17), discussed above for the density range $10^9 \text{ cm}^{-2} \leq n_{2d}^{\max} \leq 3 \times 10^{10} \text{ cm}^{-2}$, i.e. (i) strongly nonlinear increase of $1/\tau_{\text{rise}}$ with n_{2d}^{\max} (experiment) against $1/\tau_{\text{rise}}$ nearly independent of n_{2d}^{\max} (theory) and (ii) complete disappearance of the PL-jump for $n_{2d}^{\max} \simeq 10^9 \text{ cm}^{-2}$ (experiment) against a well-developed PL-jump with $\delta_{\text{PL}} \simeq 2$ for the same concentration of indirect excitons (theory), can naturally be explained by the screening effect discussed in section 4. Indeed, for low concentrations of indirect excitons, $n_{2d} \sim 10^9 \text{ cm}^{-2}$, the mean-field potential responsible for the screening effect is weak, $U_{\text{mf}} = u_0 n_{2d} \sim 0.1\text{--}0.2 \text{ meV}$. The latter value is much less than a typical amplitude of the in-plane random potential $U_{\text{QW}} = U_{\text{rand}}(\mathbf{r}_{\parallel})$: in high-quality GaAs coupled QWs one has $|U_{\text{rand}}(\mathbf{r}_{\parallel}) - \langle U_{\text{rand}} \rangle| \simeq 0.5 \text{ meV}$. Thus for $n_{2d} \sim 10^9 \text{ cm}^{-2}$ the low-energy indirect excitons are localized, i.e. the corresponding density of states cannot be approximated by the step-function $[(2M_x)/(\pi\hbar^2)]\Theta(E)$ with a sharp edge at zero energy. The Gaussian-like density of disorder-induced low-energy localized states with no well-defined energy minimum effectively suppresses the PL-jump effect. The model used in our study is not applicable to this case: a more adequate description of the thermalization and PL kinetics deals with phonon-assisted hopping between the localized states, the PL Stokes shift, etc [18, 19]. In the meantime, as we have already discussed in section 4, for $n_{2d} \geq 10^{10} \text{ cm}^{-2}$ the narrowing effect is well-developed. In this case U_{rand} is completely screened by dipole-dipole interacting indirect excitons, so that our approach is relevant to model the experimental data. Thus we explain the observed strong increase of the PL rise rate, $1/\tau_{\text{rise}}$, and the PL-jump contrast, δ_{PL} , with increasing n_{2d}^{\max} by a gradual building up of the narrowing effect, rather than by the bosonic stimulation effect.

6. Heating and cooling of indirect excitons due to the optical evaporation

Evaporative cooling or heating of indirect excitons is due to the resonant optical decay of indirect excitons in coupled QWs. In contrast with the evaporative cooling schemes designed and used in atomic optics in order to remove high-energy atoms from magnetic traps [20, 21], the optical evaporation of QW excitons is an inherent process, which deals with the low-energy particles, $0 \leq E \leq E_\gamma$ (see figure 1), from the radiative zone $|\mathbf{p}_\parallel| \leq k_0$. In the presence of a high-intensity pump pulse, the incoming, photogenerated particles effectively heat the system of indirect excitons, as was discussed in section 5. This process absolutely dominates over the optical decay of low-energy indirect excitons, so that $S_T > 0$ is determined by the first term $\propto \Lambda_{T_0}$ in the numerator of equation (18). After the pump pulse, however, the thermalization kinetics is affected by the resonant optical decay of indirect excitons. In this case, i.e. for $t \geq t_0 + \tau_{\text{pulse}}$, $\Lambda_{T_0} = 0$ and S_T is given by the second term in equation (18). Both signs of S_T can be realized: $S_T < 0$ ($S_T > 0$) corresponds to evaporative cooling (heating) of indirect excitons. Note that in our first modelling of the PL dynamics [3] this mechanism has not been considered.

In order to analyse the influence of the optical evaporation on the thermalization kinetics of indirect excitons, we compare an average thermal energy per particle, $\varepsilon_{\text{kin}}^{(2d)} = \langle E \rangle \equiv \langle (\hbar^2 p_\parallel^2) / (2M_x) \rangle$, and average energy per particle, removed from the system due to the optical decay, $\varepsilon_{\text{opt}}^{(2d)}$:

$$\varepsilon_{\text{kin}}^{(2d)} = \frac{T^2}{T_0} I_1(T, T_0) \quad \text{and} \quad \varepsilon_{\text{opt}}^{(2d)} = E_\gamma \frac{\tau_{\text{opt}}}{\tau_{\text{opt}}^E}, \quad (21)$$

where the integral I_1 , τ_{opt} and τ_{opt}^E are given by equations (19), (10) and (20), respectively.

For Maxwell–Boltzmann distributed excitons, when $k_B T$ is much larger than $k_B T_0$ and E_γ , equations (21) yield

$$\varepsilon_{\text{kin}}^{(2d)} = k_B T \left(1 - \frac{1}{4} \frac{T_0}{T} \right) \simeq k_B T \quad \text{and} \quad \varepsilon_{\text{opt}}^{(2d)} = \frac{3}{5} E_\gamma. \quad (22)$$

Thus one has $\varepsilon_{\text{kin}}^{(2d)} \gg \varepsilon_{\text{opt}}^{(2d)}$, i.e. the optical decay of low-energy QW excitons with the following re-thermalization (re-equilibration) process, due to exciton–exciton scattering, results in a net heating effect. In this case, in equations (17) S_T is positive. Because only a very small fraction of indirect excitons decay into the bulk photon modes, the heating effect is weak. For example, for $n_{2d}^{\text{max}} = 3.7 \times 10^{10} \text{ cm}^{-2}$ and $T_b = 4 \text{ K}$ the heating effect results in $\Delta T \simeq 6.4 \text{ mK}$, and for $T_b = 1.6 \text{ K}$ and $n_{2d}^{\text{max}} = 2.9 \times 10^{10} \text{ cm}^{-2}$ one estimates $\Delta T \simeq 0.016 \text{ K}$.

For a quantum degenerate quasi-2D gas of indirect excitons, when $k_B T$ is much smaller than $k_B T_0$ and E_γ , equations (21) give

$$\varepsilon_{\text{kin}}^{(2d)} \simeq \varepsilon_{\text{opt}}^{(2d)} \simeq \frac{\pi^2}{6} k_B \frac{T^2}{T_0}. \quad (23)$$

In this case one has a net cooling effect, and S_T in equations (17) is negative. According to equation (23), $\varepsilon_{\text{kin}}^{(2d)} \simeq \varepsilon_{\text{opt}}^{(2d)}$, so that the variation $\delta(T^2/T_0)$ is equal to zero. Thus $\delta n_{2d} < 0$, due to the optical decay, results in $\delta T < 0$. For $T \ll T_0$, E_γ/k_B nearly all the indirect excitons are accumulated in the radiative zone $|\mathbf{p}_\parallel| \leq k_0$, i.e. they continuously decay into the bulk photon modes. However, an average decay rate of L- and T-polarized excitons increases with increasing p_\parallel from 0 towards k_0 . In other words, one has a more effective optical removal of ‘high-energy’ indirect excitons in comparison with the optical decay of ground-state excitons. This is the underlying physical picture of the cooling effect. In order to illustrate an efficiency of

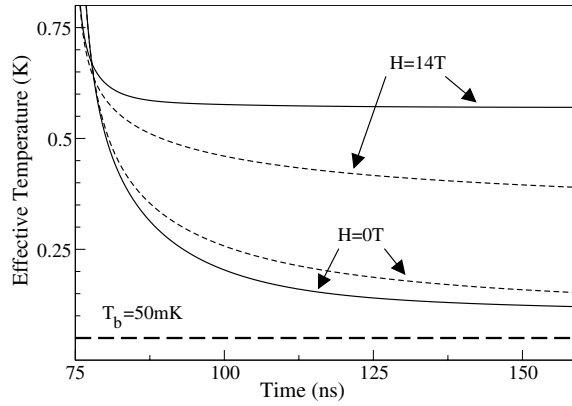


Figure 8. Thermalization dynamics, i.e. the exciton temperature $T = T(t)$, after the excitation pulse (see also figure 6(d)). The parameters used in the numerical calculations with equations (17) are the same as for figure 6. The cooling (heating) effect due to the optical evaporation of indirect excitons: $H_{\perp} = 0$ ($H_{\perp} = 14$ T). For comparison, $T = T(t)$ calculated with no influence of the optical decay on the thermalization dynamics (in equations (17) and (18) one puts $S_T = 0$ for $t \geq t_0 + \tau_{\text{pulse}}$) is shown by the dashed curves.

the evaporative optical cooling effect, in figure 7 we plot the population dynamics of the ground-state mode, $N_{E=0} = N_{E=0}(t)$, calculated with and without the S_T -term in equations (17) for $n_{2d}^{\text{max}} = 9.5 \times 10^{11} \text{ cm}^{-2}$ and $T_b = 0.05$ K.

By applying a strong magnetic field H_{\perp} one can change the exciton in-plane mass M_x , and, therefore, decrease $E_{\gamma} \propto 1/M_x$. The thermalization dynamics after the pump pulse, i.e. for $t \geq t_0 + \tau_{\text{pulse}}$, are plotted in figure 8 for $H_{\perp} = 0$ and $H_{\perp} = 14$ T. The parameters used in the calculations with equations (17) are the same as those used for figure 6. For comparison, $T = T(t)$ calculated with no evaporative heating or cooling ($S_T = 0$) is also shown. As one can see from figure 8, the evaporative optical cooling effect, which occurs at $H_{\perp} = 0$, changes into effective heating at $H_{\perp} = 14$ T. In the latter case, the evaporative optical heating effect is very strong: the exciton temperature stabilizes at $T \simeq 0.58$ K $\gg T_b = 0.05$ K. This is because by applying H_{\perp} one reduces E_{γ} to $E_{\gamma}(H_{\perp} = 14 \text{ T}) \simeq 14 \mu\text{eV}$, so that $E_{\gamma}(H_{\perp} = 14 \text{ T})/k_B \simeq 0.17$ K becomes much less than $T \simeq 1.25$ K and $T_0 \simeq 0.86$ K at the end of the excitation pulse (see figure 6).

7. Conclusions

In this paper we have analysed and numerically simulated the thermalization and photoluminescence dynamics of indirect excitons in GaAs/AlGaAs coupled QWs at very low bath temperature, $T_b \rightarrow 0$, aiming to model the data of recent optical experiments [3] performed at extremely low cryostat temperature, $T_b = 50$ mK. The following conclusions summarize our study.

- (i) The observed PL-jump cannot unambiguously be attributed to bosonic stimulation of the scattering processes into the ground-state mode $\mathbf{p}_{\parallel} = 0$. According to our calculations, for the concentrations $n_{2d}^{\text{max}} \leq 3 \times 10^{10} \text{ cm}^{-2}$, relevant to the experiments [2, 3], the PL-jump is mainly due to classical cooling of indirect excitons right after the trailing edge of the rectangular excitation pulse.
- (ii) The narrowing effect, i.e. an effective screening of the in-plane disorder-induced random potential U_{QW} by dipole-dipole interacting indirect excitons, naturally explains the

strongly nonlinear dependence of the PL rise time, $\tau_{\text{rise}} = \tau_{\text{rise}}(n_{2d}^{\text{max}})$, and PL-jump contrast, $\delta_{\text{PL}} = \delta_{\text{PL}}(n_{2d}^{\text{max}})$, observed for $10^9 \text{ cm}^{-2} \leq n_{2d}^{\text{max}} \leq 3 \times 10^{10} \text{ cm}^{-2}$.

- (iii) In the presence of classical and quantum slowing down of the thermalization processes and continuous resonant optical decay of indirect excitons, the maximum occupation numbers of the ground-state mode are still rather small, $N_{E=0} \sim 10$ for $n_{2d}^{\text{max}} \simeq 3 \times 10^{10} \text{ cm}^{-2}$ and $N_{E=0} \sim 100$ for $n_{2d}^{\text{max}} \simeq 10^{11} \text{ cm}^{-2}$. While the thermalization and PL dynamics are already affected by nonclassical statistics, the above values of $N_{E=0}$ are probably too small to initiate the BEC or BEC-like phase transition.
- (iv) Optical evaporation of low-energy indirect excitons strongly influences the thermalization kinetics. The optical decay results in the heating of QW excitons, if $k_{\text{B}}T \geq E_{\gamma}$ and $k_{\text{B}}T_0$, and in the effective cooling, if $k_{\text{B}}T \ll E_{\gamma}$ and $k_{\text{B}}T_0$.

The relaxation thermodynamics used in our analysis (see equations (4) and (17)) still gives a simplified description of the thermalization kinetics of indirect excitons. A first-principle numerical modelling within a quantum Boltzmann equation, which explicitly includes both QW exciton—QW exciton and QW exciton—bulk LA-phonon scattering processes, is in progress and will be published elsewhere [22].

Acknowledgments

The author appreciates valuable discussions with L V Butov, D S Chemla, P B Littlewood, B D Simons, L E Smallwood, D W Snoke and A V Soroko. Support of this work by the EU RTN Project HPRN-CT-2002-00298 ‘Photon-Mediated Phenomena in Semiconductor Nanostructures’ is gratefully acknowledged.

References

- [1] Snoke D 2002 *Nature* **298** 1368
- [2] Butov L V, Imamoglu A, Mintsev A V, Campman K L and Gossard A C 1999 *Phys. Rev. B* **59** 1625
- [3] Butov L V, Ivanov A L, Imamoglu A, Littlewood P B, Shashkin A A, Dolgoplov V T, Campman K L and Gossard A C 2001 *Phys. Rev. Lett.* **B 86** 5608
- [4] Lozovik Yu E and Ruvinskii A M 1997 *Zh. Eksp. Teor. Fiz.* **112** 1791
Lozovik Yu E and Ruvinskii A M 1997 *JETP* **85** 979 (Engl. Transl.)
- [5] Butov L V, Lai C W, Chemla D S, Lozovik Yu E, Campman K L and Gossard A C 2001 *Phys. Rev. Lett.* **87** 216804
- [6] Lozovik Yu E, Ovchinnikov I V, Volkov S Yu, Butov L V and Chemla D S 2002 *Phys. Rev. B* **65** 235304
- [7] Golub J E, Kash K, Harbison J P and Florez L T 1990 *Phys. Rev. B* **41** 8564
- [8] Alexandrou A, Kash J A, Mendez E E, Zachau M, Hong J M, Fukuzawa T and Hase Y 1990 *Phys. Rev. B* **42** 9225
- [9] Szymanska M H and Littlewood P B 2003 *Phys. Rev. B* **67** 193305
- [10] Ivanov A L 2002 *Europhys. Lett.* **59** 586
- [11] Ivanov A L, Littlewood P B and Haug H 1999 *Phys. Rev. B* **59** 5032
- [12] Ivanov A L, Ell C and Haug H 1997 *Phys. Rev. E* **55** 6363
- [13] Ell C, Ivanov A L and Haug H 1998 *Phys. Rev. B* **57** 9663
- [14] Soroko A V and Ivanov A L 2002 *Phys. Rev. B* **65** 165310
- [15] Iordanski S V and Kashuba A 2001 *Pis. Zh. Eksp. Teor. Fiz.* **73** 542
Iordanski S V and Kashuba A 2001 *JETP Lett.* **73** 479 (Engl. Transl.)
- [16] Soroko A V, Ivanov A L and Butov L V 2002 *Phys. Status Solidi a* **190** 719
- [17] Krauth W, Trivedi N and Ceperley D 1991 *Phys. Rev. Lett.* **67** 2307
- [18] Baranovskii S D, Eichmann R and Thomas P 1998 *Phys. Rev. B* **58** 13081
- [19] Runge E 2002 *Solid State Phys.* **57** 149
- [20] Davis K B, Mewes M-O, Joffe M A, Andrews M R and Ketterle W 1995 *Phys. Rev. Lett.* **74** 5202
- [21] Ketterle W 2002 *Rev. Mod. Phys.* **74** 1131
- [22] Smallwood L E and Ivanov A L 2004 unpublished